PALEOANTHROPOLOGY

The growth pattern of Neandertals, reconstructed from a juvenile skeleton from El Sidrón (Spain)

Antonio Rosas,[1]*† Luis Ríos,[1,2]† Almudena Estalrrich,[1,3] Helen Liversidge,[4] Antonio García-Tabernero,[1] Rosa Huguet,[5] Hugo Cardoso,[6] Markus Bastir,[1] Carles Lalueza-Fox,[7] Marco de la Rasilla,[8] Christopher Dean[9]

Ontogenetic studies help us understand the processes of evolutionary change. Previous studies on Neandertals have focused mainly on dental development and inferred an accelerated pace of general growth. We report on a juvenile partial skeleton (El Sidrón J1) preserving cranio-dental and postcranial remains. We used dental histology to estimate the age at death to be 7.7 years. Maturation of most elements fell within the expected range of modern humans at this age. The exceptions were the atlas and mid-thoracic vertebrae, which remained at the 5- to 6-year stage of development. Furthermore, endocranial features suggest that brain growth was not yet completed. The vertebral maturation pattern and extended brain growth most likely reflect Neandertal physiology and ontogenetic energy constraints rather than any fundamental difference in the overall pace of growth in this extinct human.

Neandertals provide us with an important perspective on our own biology (*1*). Both modern humans and Neandertals arose from a recent common ancestor along independent evolutionary lines, becoming large-brained hominins but with contrasting body forms. Developing a large brain is energetically expensive and places a constraint on somatic growth (*2*). The unusually high cost of modern human brain development is greatest during the infant and childhood periods and seems to require a compensatory slowing of childhood body growth (*2*, *3*). Neandertals had larger average cranial capacity than modern humans, but little is known about the ontogenetic trajectories of brain and body underlying this difference.

Some studies have proposed that a larger brain in Neandertals can be explained by a faster rate of early postnatal growth (*4*), yet others have proposed a longer period of growth as an explanation (*5*, *6*). However, in large-brained hominins like modern humans and Neandertals, an accelerated pace of brain growth, coincident with accelerated somatic growth, would impose a high energetic cost (*2*). Yet the trade-off between the different aspects of somatic and neural growth in Neandertals, particularly during the juvenile period, remains unclear.

Here we describe a partial juvenile Neandertal skeleton from the 49-thousand-year-old site of El Sidrón (Asturias, Spain). The specimen has a mixed dentition of deciduous and permanent teeth and preserves cranial, dental, and postcranial remains (Figs. 1 and 2A and supplementary text 1 and 2), providing a rare opportunity to estimate an age at death from daily dental incremental markings preserved in teeth, against which to compare many aspects of its dento-skeletal maturation. Chronological age is fundamental for assessing patterns of maturation in different dento-skeletal systems, both within individuals and between species. This approach allowed us to ask what the probability is that this specimen would fit within or lie beyond the ranges of modern human variation and represent its own pattern of dental and skeletal maturation.

The El Sidrón cave system (Asturias, Spain) (Fig. 1C and supplementary text 1) has provided more than 2500 remains of seven adults and six immature individuals belonging to a single Neandertal group (*7*) with close kinship relations (*8*). Among them, a partial immature skeleton was recovered with up to ~36% (left side) preserved. Virtually all of the remains associated with this individual come from the 1-m^2 G-6 square grid of the archaeological site (supplementary text 2), and importantly, several were found in anatomical association. From the three mitochondrial DNA lineages detected within this Neandertal group, this individual belongs to line C of the group and was tentatively identified as the child of adult female 4 and the older sibling of infant 1 (*8*).

A number of diagnostic Neandertal features are present throughout the skeleton (supplementary text 2). Although ancient DNA failed to confirm the sex, group-specific evaluation of canine size and bone robusticity strongly suggests that it was male (supplementary text 2). Dental development, with a near-complete first molar (M1) root, would place him in the juvenile stage of hominin life history (*3*). Height and weight estimates indicate that he was a sturdy individual, weighing ~26 kg and standing ~111 cm tall at the time of death (supplementary text 2). Biosocial markers indicate that El Sidrón juvenile 1 (J1) was right-handed, with evidence that he was involved with, or learning, adult behaviors and economic activities (*9*). Apart from mild linear dental enamel hypoplasia around the age of 2 to 3 years, there is no other evidence of pathology. Several postmortem cut marks appear on some of the bones.

Age at death was first established by dental histology. Daily incremental markings in two sections of El Sidrón J1 first left upper molar (see materials and methods, figs. S1 and S2, and supplementary text 3) were used to estimate an average age at death of 7.69 years (range: 7.61 to 7.78 years). Biological maturity was then assessed using modern human references for dental, skeletal, and somatic maturation (supplementary text 4 to 7).

Dental maturity was assessed in two ways. Individuals from two reference samples of modern children of known age (n = 4072 and 6829) were assigned a radiographic stage of development for each tooth (supplementary text 4). Compared with the first sample, dental maturity of El Sidrón J1 was judged to be 71.7 to 72.1% complete. Probability density plots for mean age of transition entering each tooth stage were computed from the second sample, and El Sidrón J1 fell well within the modern human range for all tooth types represented (Fig. 2B). Skeletal maturity (SM) and skeletal age (SA) were assessed from six secondary ossification centers from the elbow, hand, wrist, and knee, by applying established pediatric methods (figs. S3 to S5 and supplementary text 5). The SA interval ranged from 6 to 10 years, with an average of 7.62 ± 2 years (table S7). Maturity of each individual vertebra was assessed in two ways. Individuals from a sample of 106 immature modern human skeletons (of which 70 were of known age and sex) were assigned a stage of fusion of the neurocentral synchondrosis (NS) and a radiographic stage of development for the lower M1 (materials and methods). Probability density functions for the mean age of transition entering fusion of the NS of the first cervical vertebra (C1) and the 3rd to 11th thoracic vertebrae (T3 to T11) were computed from the known age sample (Fig. 2C). The same procedure was applied to the total sample using the mean age entering the respective M1 stage scored (Fig. 2D). Compared with chronological and dental age,

[1]Paleoanthropology Group, Department of Paleobiology, Museo Nacional de Ciencias Naturales (MNCN)–Consejo Superior de Investigaciones Científicas (CSIC), Calle José Gutiérrez Abascal 2, 28006 Madrid, Spain. [2]Department of Physical Anthropology, Aranzadi Society of Sciences, Zorroagagaina 11, 20014 Donostia–San Sebastián, Gipuzkoa, Spain. [3]Department of Paleoanthropology, Senckenberg Research Institute and Natural History Museum Frankfurt, Senckenberganlage 25, 60325 Franckfurta, Germany. [4]Queen Mary University of London, Institute of Dentistry, Turner Street, London E1 2AD, UK. [5]Institut Català de Paleoecologia Humana i Evolució Social–Unidad Asociada al CSIC, Campus Sescelades (Edifici W3), Universitat Rovira i Virgili, Carrer Marcel.lí Domingo s/n, 43007 Tarragona, Spain. [6]Department of Archaeology, Simon Fraser University, Burnaby, British Columbia V5A1S6, Canada. [7]Institute of Evolutionary Biology (CSIC–Universitat Pompeu Fabra), Carrer Dr. Aiguader 88, 08003 Barcelona, Spain. [8]Área de Prehistoria Departamento de Historia, Universidad de Oviedo, Calle Teniente Alfonso Martínez s/n, 33011 Oviedo, Spain. [9]Department of Cell and Developmental Biology, University College London, Gower Street, London WC1E 6BT, UK.
***Corresponding author. Email: arosas@mncn.csic.es** †These authors contributed equally to this work.

maturation of each available vertebra of El Sidrón J1 fell at the extreme end of the modern human range (fig. S6 and supplementary text 6). SM of El Sidrón J1 vertebral column [fused C3-C5-C6, T1-T2, and L2-L3 (second and third lumbar vertebrae); unfused C1 and four middle thoracic vertebrae] fits the modern human observed sequence of NS vertebral fusion but corresponds chronologically to younger individuals between 4 to 6 years of age (Fig. 2C). Percentage of adult size (PAS) attained (*10*) was calculated as a measure of somatic maturation for 53 measurements through the cranial, axial, and appendicular skeleton (supplementary text 7). In comparison with a sample of 11 modern human skeletons with chronological age (CA) between 6.5 and 8.5 years, values of El Sidrón J1 fell within (49 variables) or very close to (4 variables) the modern human range (Fig. 3A). The height-for-age of El Sidrón J1 also fell within the range of modern humans (*11*) (Fig. 3B), with Neandertal body shape features already observable at 7.7 years (*12*, *13*) (Fig. 3C).

Clearly visible bone resorption areas on the inner aspect of the occipital poles provide some evidence that brain expansion was still ongoing (Fig. 4 and supplementary text 8). Resorption activity is a characteristic of the period of brain growth in modern humans (*14*). These observations suggest that specific locations on the occipital lobe and cerebellum of El Sidrón J1 were still increasing in size. The extremely well-defined imprints of the gyri and sinus impressions on the internal aspect of SD-2300, as well as the narrow dural sinus grooves (supplementary text 8), further suggest that the encephalon was still exerting growing pressure on the neurocranium.

A consensus value for endocranial volume of ~1330 cm^3 (supplementary text 8) was computed, which represents ~87.5% of mean Neandertal adult endocranial volume (1520 cm^3). On average, modern humans achieve 90% of adult brain weight by 5 years old (*15*) and 95% by 7 years (*16*). This suggests that further brain growth in El Sidrón J1 would likely have continued beyond the time expected in modern humans at 7.7 years.

The dental and skeletal maturity of El Sidrón J1 were compared with modern humans. Dental development is what one would expect for a child of his age. This contrasts with previous findings from isolated cranio-dental material that have reported a faster pace of dental development (*17*, *18*). Compared with early *Homo* specimens at a comparable stage of dental development, El Sidrón J1 is at least 2.7 years older than a ~2-million-year-old *Homo* specimen, StW 151 (*19*–*22*), but almost identical in age (7.78 years) to a 315-thousand-year-old *Homo sapiens* specimen from Jebel Irhoud, Morocco (*23*), that shows a prolonged modern human–like period of dental developmental (*24*). At 7.7 years of age, El Sidrón J1 shows a second incisor (I2) at the stage of alveolar eruption, an M2 at the stage of crown completion, and an M3 crypt present in the mandible. It is, therefore, no longer possible to assume that these events occurred earlier at ~6 years of age, or that M2 erupted at 8 years of age, in all Neandertals (*18*).

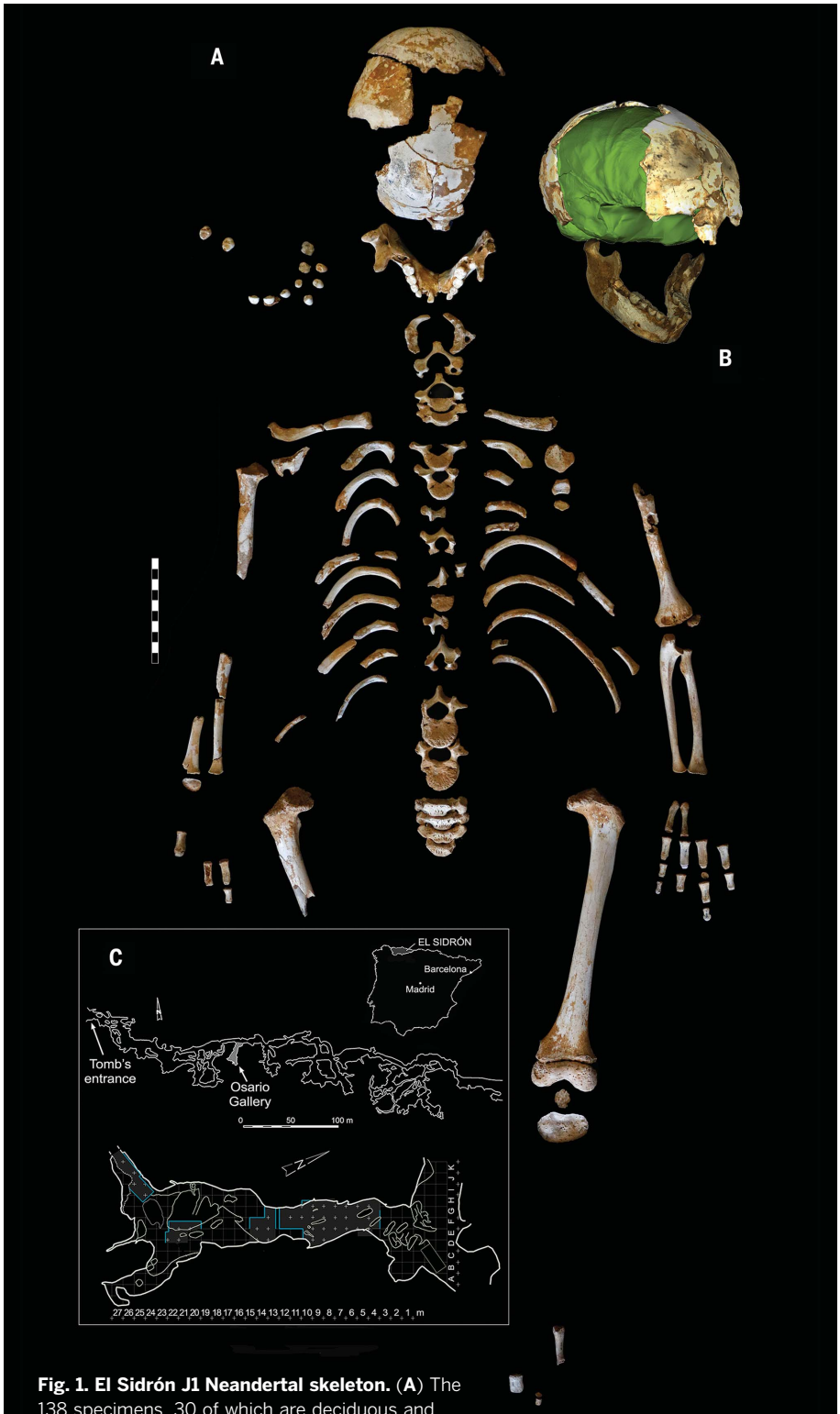

Fig. 1. El Sidrón J1 Neandertal skeleton. (**A**) The 138 specimens, 30 of which are deciduous and permanent teeth, that compose the El Sidrón J1 skeleton. Cranial, axial, and appendicular elements are well represented, but the legs (especially the right one) are less well represented. (**B**) Virtual reconstruction of the El Sidrón J1 skull and endocast based on the same cranial bone specimens shown in (A). (**C**) Localization of the El Sidrón site in the Iberian Peninsula (Asturias, Spain). A map of the karst system depicts the 25-m-long Osario gallery (shadowed), as well as the excavated area of this gallery. Most of the specimens of El Sidrón J1 were recovered from the G-6 1-m^2grid of the excavation.

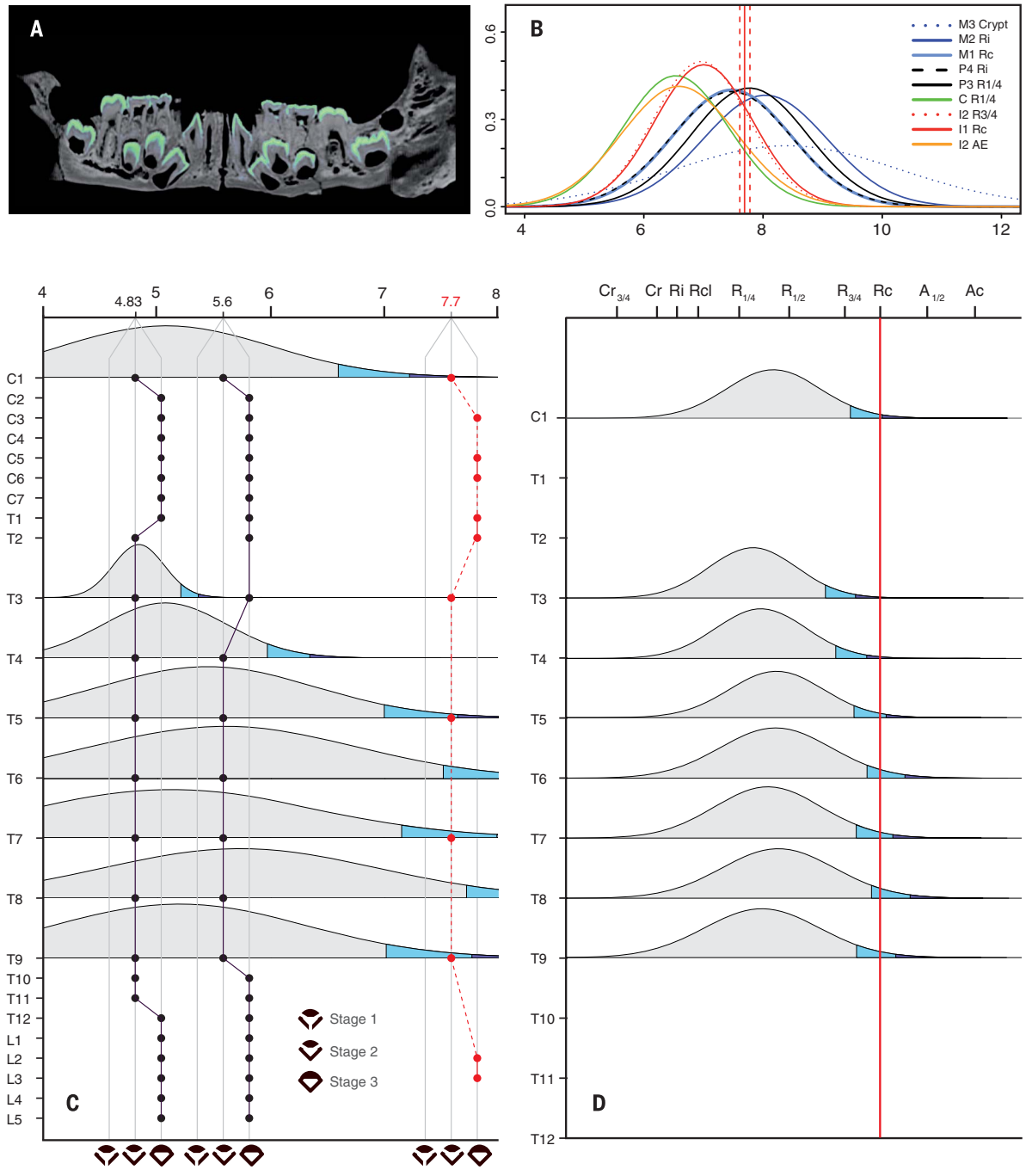

Fig. 2. Dental and vertebral maturation of El Sidrón J1. (**A**) Computed tomography (CT) scan image of the mandible of El Sidrón J1, with the enamel shown in green. (**B**) Probability density plots (PDPs) for mean age of transition entering each mandibular tooth stage scored for El Sidrón J1 in a radiographic sample (n = 6829 individuals) of modern children of known chronological age (CA). Red vertical lines represent the CA of El Sidrón J1 from dental histology (7.69 years; range: 7.61 to 7.78 years). (**C**) Maturation of the spine relative to CA in El Sidrón J1 and modern humans. The vertical axis represents the presacral vertebral column; the horizontal axis represents age in years. For each vertebra, the three successive maturation stages are represented (see vertebral diagrams in the figure): stage one, unfused posterior synchondrosis (PS) and neurocentral synchondrosis (AS); stage two, fused PS and unfused neurocentral synchondrosis (NS); stage three, fused PS and NS. A sample of 70 known CA skeletons was used to develop PDPs for mean age of transition entering fusion of the NS for each vertebra (from stage two to three). El Sidrón J1 is displayed in red, and the two oldest modern human cases (4.83 and 5.6 years) with a spine maturation similar to that of El Sidrón J1 (unfused C1 and middle thoracic vertebrae) are represented in black. The C1 falls within the P = 0.01 shaded area of the PDP, whereas the thoracic vertebrae would fall outside (T3 and T4), in the P = 0.05 shaded area (T5, T6, T7, and T9), or under the PDP (T8). (**D**) Maturation of the spine relative to dental maturation in El Sidrón J1 and in modern humans. The vertical axis represents C1 and the thoracic vertebrae, whereas stages of formation of the first permanent mandibular molar are represented on the horizontal axis. A sample of 106 modern human skeletons of diverse origins was used to develop PDPs for mean first molar formation stage entering fusion of the NS for each vertebra (from stage two to three). The vertical red line, representing complete root formation of the first permanent molar of El Sidrón J1, falls in the P = 0.05 area in all PDPs.

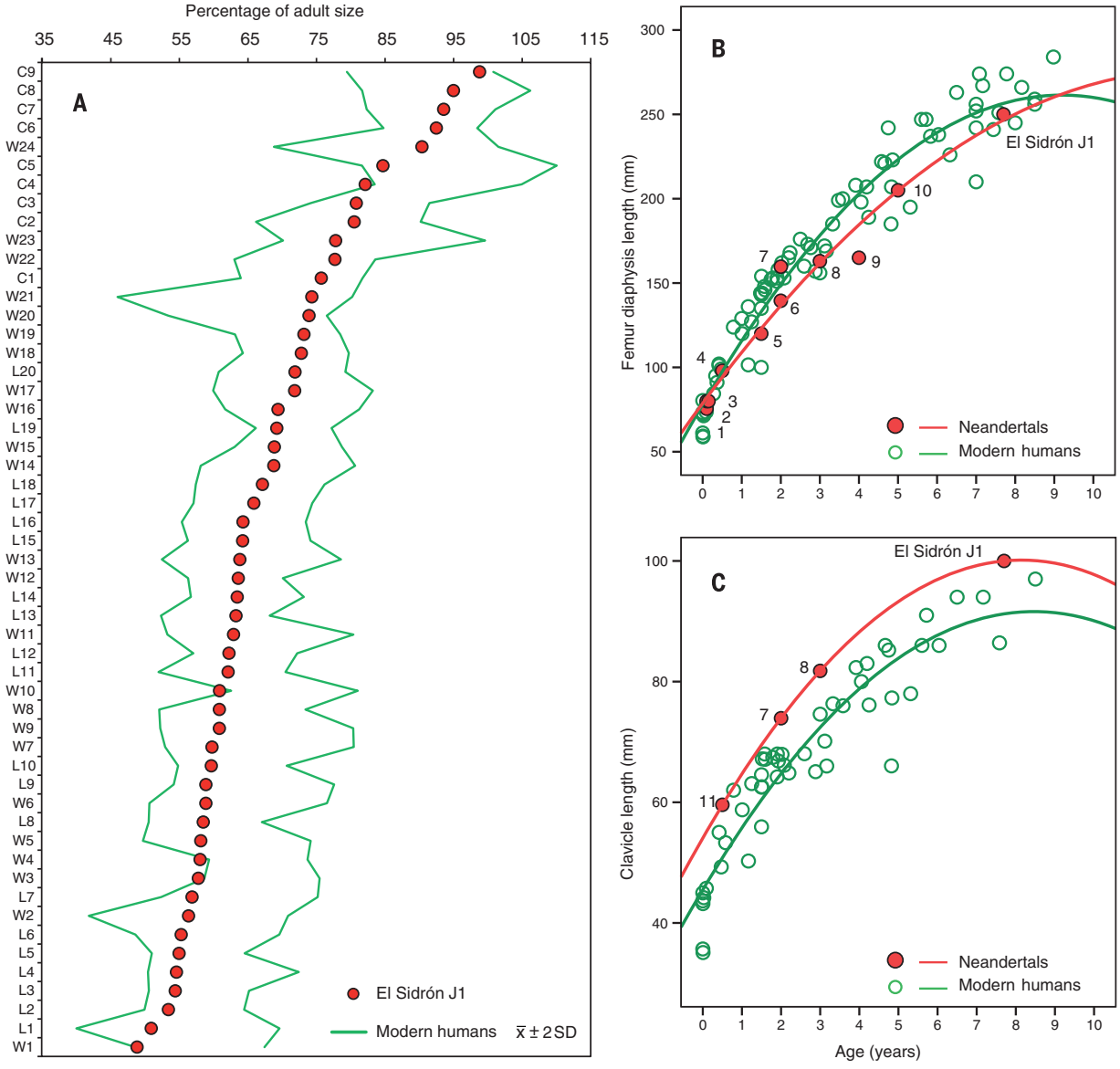

Fig. 3. Somatic maturation and size-by-age of El Sidrón J1. (**A**) Percentage of adult size (PAS) of El Sidrón J1 in comparison with 11 modern human skeletons with CA between 6.5 and 8.5 years (supplementary text 7). L, length variables, including bones from the appendicular and axial skeleton contributing to stature (i.e., vertebral body height); W, width variables, including diaphysis and epiphysis from the appendicular and axial (articular widths, diaphyseal circumferences, vertebral body widths); C, craniofacial and central nervous system–associated variables from cranial bones, mandible, and vertebrae. Variables are listed in supplementary text 7. (**B**) Femoral lengths of El Sidrón J1 and a Neandertal ontogenetic series (*17*), with 80 modern human skeletons with CA of 0 to 9 years, with fitted quadratic models (Neandertals, R^2 = 0.968; modern humans, R^2 = 0.952). (**C**) Clavicle length of El Sidrón J1 and a Neandertal ontogenetic series (*18*), with 51 modern human skeletons with CA of 0 to 9 years, with fitted quadratic models (Neandertals, R^2 = 1; modern humans, R^2 = 0.889). 1, La Ferrassie 4/Le Moustier 2; 2, La Ferrassie 4b/La Ferrassie 4; 3, Mezmaiskaya; 4, Kiik-Koba 2; 5, Shanidar 10; 6, Dederiyeh 2; 7, Dederiyeh 1; 8, Roc de Marsal 1; 9, La Ferrassie 6; 10, Cova Negra; 11, Amud 7.

As with El Sidrón J1, new ages at death (*18*) for younger Neandertal specimens (Engis 2, Gibraltar 2, Krapina B, and Obi-Rakhmat 1) fall within modern ranges, but two older specimens, Scladina and Le Moustier 1 (*18*, *25*), now seem unexpectedly young. An assumed early age, 2155 days (*18*), of initial M3 mineralization (*18*, *25*) or foreshortened estimates of root formation times (*26*) might explain this. Clearly, variation in Neandertal dental development would have been as great as today but may generally have tended toward the more advanced end of the modern human spectrum.

A *Homo erectus* juvenile aged between 7.6 to 8.8 years (KNM WT 15000) shows evidence of both advanced dental development and earlier attainment of body mass and stature than is typical of modern humans of a similar age (*22*, *27*). However, SA and PAS are also within the modern range, given the limited level of biological resolution of SA and PAS estimation. Growth and development in this juvenile Neandertal fit the typical features of human ontogeny, where there is slow somatic growth between weaning and puberty (*3*, *28*) that may offset the cost of growing a large brain. Moreover, a slower pace of growth provides an opportunity for shifts in both the rate and timing of brain growth (*4*–*6*, *15*). Even so, divergent morphogenetic trajectories underlying shape differences, such as brain development (*29*–*31*) and cranio-facial morphology (*32*, *33*), can exist within this broadly human growth pattern.

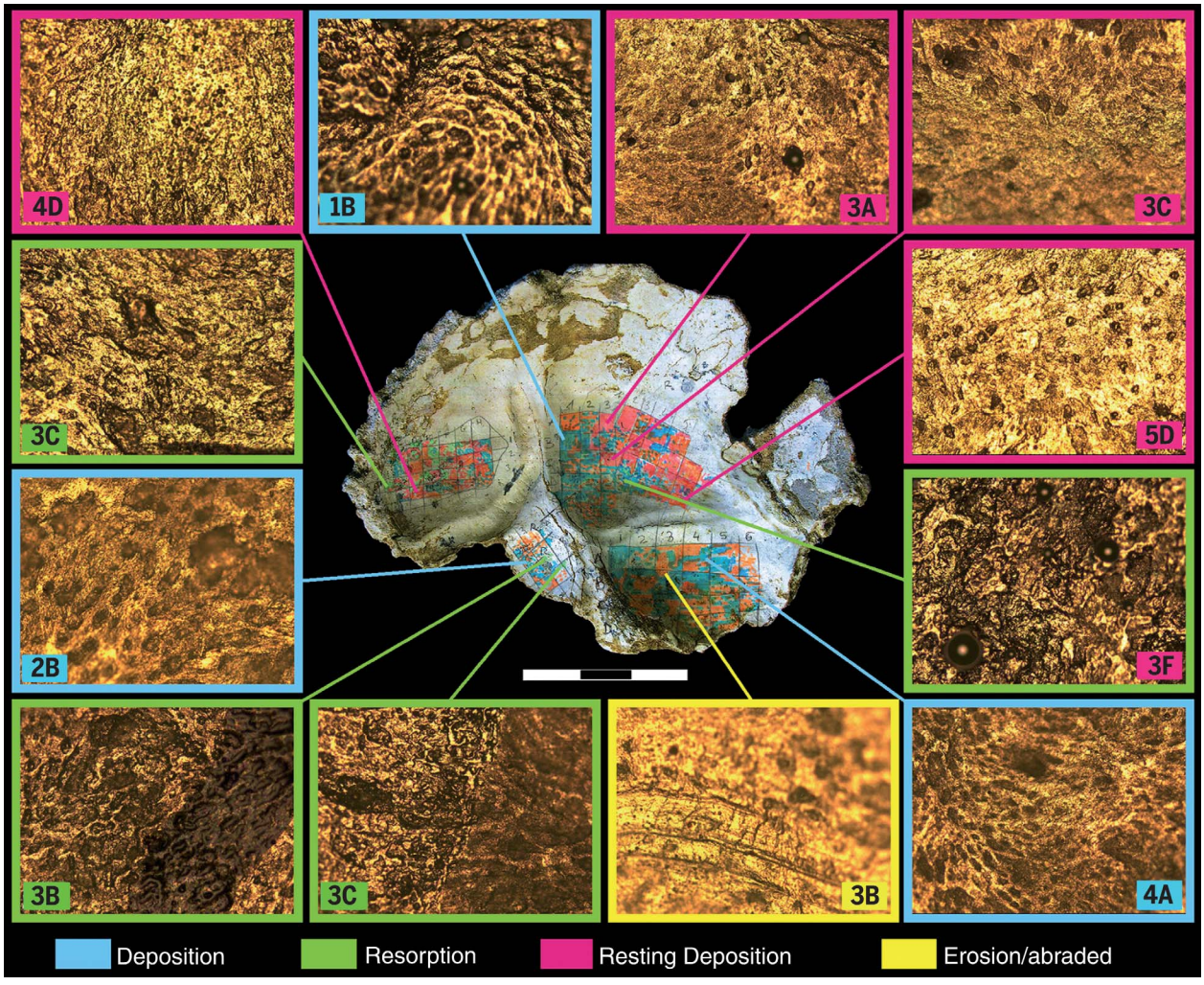

Fig. 4. Occipital bone of El Sidrón J1 with reference grid and color-coded remodeling activity map superimposed. All pictures were taken with a light-reflected microscope at 20× magnification. Each image is framed with its corresponding color code of histological activity (blue, bone deposition; pink, bone resting deposition; green, bone resorption; orange, erosion/abrasion of taphonomic origin) and connected to its anatomical location. The alphanumeric legend indicates grid reference. During the process of growth remodeling, osteoblastic activity (formation: blue color) usually exceeds osteoclastic activity (resorption: green color), resulting in differential growth of the bone. Deposition areas are characterized by the presence of collagen fiber bundles and insertion of Sharpey's fibers, whereas resorption areas are recognized as anisotropic resorption bays (Howship's lacunae). Bone deposition (blue) is easily illustrated by collagen fiber bundles, at times changing direction to form a wavy impression (1B and 4A). Resting deposition can be identified by a dense and uniform bright surface in which the deposition of bone matrix masks other histological features, including collagen fiber and Sharpey's fibers (4D and 5D). Insertions of Sharpey's fibers are spread out over the deposition surfaces (2B and 5D). A well-defined reversal line can be seen in 3C, and an example of taphonomic alteration (e.g., scratches) is depicted in 3B. Scale bar (bottom of central panel), 3 cm.

The one divergent aspect of ontogeny is the timing of maturation within the vertebral column. In all hominoids, the NS of the middle thoracic vertebrae and the atlas are the last to fuse, but in this Neandertal, it appears that fusion occurs ~2 years later than in modern humans (or closer to M1 root closure than to the M1 root being a quarter to half formed).

At 1.5 to 2 years old, the state of maturation of the complete spine of the Dederiyeh 1 child (*34*, *35*) suggests that, earlier in ontogeny, when the posterior synchondroses fuse, Neandertals followed a vertebral maturation schedule similar to that of modern humans. The later fusion of the NS could reflect a decoupling of certain smaller-scale aspects of growth and maturation in these extinct humans in the transition from the childhood to the juvenile stage. Although the implications of this are unknown, they may be related to the characteristically expanded Neandertal torso (*36*, *37*) or to ongoing growth of the neuraxis. Together, these findings suggest that late Neandertal neural growth pattern exhibits a degree of modularity relative to dental development, something also detected in gorillas (*38*).

Clarifying differences and similarities in growth patterns between extinct humans, especially Neandertals, and modern humans helps us better define our own phylogenetic history. The distinctive pattern of vertebral maturation and extended brain growth might reflect the Neandertal physiology and ontogenetic energy constraints rather than defining a fundamental difference in the overall pace of growth in this species of *Homo*.

REFERENCES AND NOTES

1. E. Trinkaus, R. L. Tompkins, "The Neanderthal life-cycle. The possibility, probability, and perceptibility of contrasts with recent humans," in *Primate Life History and Evolution*, C. J. Derousseau, Ed. (Wiley, 1990), vol. 14, pp. 153–180.
2. C. W. Kuzawa *et al.*, *Proc. Natl. Acad. Sci. U.S.A.* **111**, 13010–13015 (2014).
3. B. Bogin, *Patterns of Human Growth* (Cambridge Univ. Press, 1999).
4. M. S. Ponce de León *et al.*, *Proc. Natl. Acad. Sci. U.S.A.* **105**, 13764–13768 (2008).

5. S. R. Leigh, *Evol. Anthropol.* **10**, 223–236 (2001).
6. S. R. Leigh, *Evol. Biol.* **39**, 587–599 (2012).
7. A. Rosas *et al.*, *Cuaternario Geomorfol.* **29**, 77 (2015).
8. C. Lalueza-Fox *et al.*, *Proc. Natl. Acad. Sci. U.S.A.* **108**, 250–253 (2011).
9. A. Estalrrich, A. Rosas, *J. Hum. Evol.* **80**, 51–63 (2015).
10. L. T. Humphrey, *Am. J. Phys. Anthropol.* **105**, 57–72 (1998).
11. J. A. Martín-González, A. Mateos, I. Goikoetxea, W. R. Leonard, J. Rodríguez, *J. Hum. Evol.* **63**, 140–149 (2012).
12. R. García-González *et al.*, *L'Anthropologie* **113**, 222–232 (2009).
13. T. D. Weaver *et al.*, *Proc. Natl. Acad. Sci. U.S.A.* **113**, 6472–6477 (2016).
14. E. F. Kranioti *et al.*, *Anat. Rec.* **292**, 1764–1770 (2009).
15. S. L. Robson, B. Wood, *J. Anat.* **212**, 394–425 (2008).
16. T. Cabana, P. Jolicoeur, J. Michaud, *Am. J. Hum. Biol.* **5**, 93–99 (1993).
17. F. V. Ramirez Rozzi, J. M. Bermudez de Castro, *Nature* **428**, 936–939 (2004).
18. T. M. Smith *et al.*, *Proc. Natl. Acad. Sci. U.S.A.* **107**, 20923–20928 (2010).
19. J. Moggi-Cecchi, P. V. Tobias, A. D. Beynon, *Am. J. Phys. Anthropol.* **106**, 425–465 (1998).
20. T. M. Smith *et al.*, *PLOS ONE* **10**, e0118118 (2015).
21. A. Le Cabec, N. Tang, P. Tafforeau, *PLOS ONE* **10**, e0123019 (2015).
22. M. C. Dean, H. M. Liversidge, *Ann. Hum. Biol.* **42**, 415–429 (2015).
23. J.-J. Hublin *et al.*, *Nature* **546**, 289–292 (2017).
24. T. M. Smith *et al.*, *Proc. Natl. Acad. Sci. U.S.A.* **104**, 6128–6133 (2007).
25. P. Tafforeau, J. P. Zermeno, T. M. Smith, *J. Hum. Evol.* **62**, 424–428 (2012).
26. L. L. Shackelford, A. E. Stinespring Harris, L. W. Konigsberg, *Am. J. Phys. Anthropol.* **147**, 227–253 (2012).
27. M. C. Dean, B. H. Smith, "Growth and development of the Nariokotome youth, KNM-WT 15000," in *The First Humans: Origin and Early Evolution of the Genus* Homo, F. E. Grine, J. G. Fleagle, R. E. Leakey, Eds. (Vertebrate Paleobiology and Paleoanthropology Series, Springer, 2009), pp. 101–120.
28. J. L. Thompson, A. J. Nelson, *Hum. Nat.* **22**, 249–280 (2011).
29. H. Coqueugniot, J.-J. Hublin, *Period. Biol.* **109**, 379 (2007).
30. P. Gunz, S. Neubauer, B. Maureille, J.-J. Hublin, *Curr. Biol.* **20**, R921–R922 (2010).
31. J.-J. Hublin, S. Neubauer, P. Gunz, *Philos. Trans. R. Soc. London Ser. B* **370**, 20140062 (2015).
32. M. S. Ponce de León, C. P. E. Zollikofer, *Nature* **412**, 534–538 (2001).
33. M. Bastir, P. O'Higgins, A. Rosas, *Proc. Biol. Sci.* **274**, 1125–1132 (2007).
34. O. Kondo, Y. Dodo, T. Akazawa, S. Muhesen, *J. Hum. Evol.* **38**, 457–473 (2000).
35. Y. Dodo, O. Kondo, S. Muhesen, T. Akazawa, in *Neandertals and Modern Humans in Western Asia* (2002), pp. 323–338.
36. R. G. Franciscus, S. E. Churchill, *J. Hum. Evol.* **42**, 303–356 (2002).
37. D. García-Martínez *et al.*, *J. Hum. Evol.* **70**, 69–72 (2014).
38. G. A. Macho, J. A. Lee-Thorp, *PLOS ONE* **9**, e102794 (2014).

ACKNOWLEDGMENTS

We thank the entire excavation team working at El Sidrón, as well as the other members of the Paleoanthropology Group of MNCN-CSIC, including S. Garcia-Vargas, J. M. Baquero, and D. Oropesa. We are grateful to the NESPOS Society and the professionals behind it, as well as to the following Institutions and scholars for providing CT data: A. Balzeau, Muséum National D'Histoire Naturelle Paris; C. Stringer and R. Krusynski, Natural History Museum, London; F. Spoor, University College London; and P. Semal, Royal Belgian Institute of Natural Sciences, Brussels. We thank H. Coqueugniot [CNRS–PACEA (De la Préhistoire à l'Actuel: Culture, Environnement et Anthropologie)] for advice on cranial reconstruction. We thank Clinica Ruber for technical support with CT scans and radiographs. We also thank the following curators and researchers for granting access to skeletal collections: J. Alves and S. García (Museu Nacional de História Natural e da Ciência, Lisbon); A. L. Santos, S. Wasterlain, T. Ferreira, and the staff of DRYAS (Universidade de Coimbra); L. Jellema (Hamann-Todd Osteological Collection); J. Pastor (Universidad de Valladolid); M. Benito (Universidad Complutense de Madrid); and E. Gilissen (Royal Museum of Central Africa; Synthesys grant BE-TAF-4580 to L.R.). We also thank B. Bogin for the discussion of several aspects of the research with L.R. (José Castillejo visiting research grant CAS16/00108 to Loughborough University). A. Martínez helped with the figures. A.R. was supported by a grant from the Ministerio de Economía y Competitividad of Spain (CGL2016-75-109-P Convenio Principado de Asturias–Universidad de Oviedo CN-09-084). We additionally thank three anonymous referees for valuable suggestions. A.R., L.R., C.D., and H.L. wrote the manuscript. All authors contributed to the manuscript and the overall interpretation. L.R., A.R., and H.C. compiled osteological databases. H.L. and C.D. provided human dental databases. A.R., L.R., A.E., R.H., A.G.-T., and M.B. performed fossil anatomical identification and numerical analyses and discussed the results. C.L.-F. and M.R. provided paleogenetic and archeological background information. Original fossils from the El Sidrón site are housed at MNCN.

SUPPLEMENTARY MATERIALS

www.sciencemag.org/content/357/6357/1282/suppl/DC1
Material and Methods
Supplementary Text 1 to 8
Figs. S1 to S24
Tables S1 to S34
References (*39–146*)

12 May 2017; accepted 27 July 2017
10.1126/science.aan6463

The growth pattern of Neandertals, reconstructed from a juvenile skeleton from El Sidrón (Spain)

Antonio Rosas, Luis Ríos, Almudena Estalrrich, Helen Liversidge, Antonio García-Tabernero, Rosa Huguet, Hugo Cardoso, Markus Bastir, Carles Lalueza-Fox, Marco de la Rasilla and Christopher Dean

Science **357** (6357), 1282-1287.
DOI: 10.1126/science.aan6463

Neandertal growth patterns

The ontogeny of different parts of the Neandertal skeleton has been derived from isolated bones and fragments. Rosas *et al.* present a more complete skeleton of a Neandertal child, aged 7 to 8 years, from a 49,000-year-old site in northern Spain. The skeleton preserves dental, cranial, and postcranial material, allowing the assessment of dental and skeletal maturation with age. Most of the elements indicate an overall growth rate similar to that of modern human children. The main difference between Neandertals and modern humans is in the vertebral column. Also, several features indicate ongoing brain growth. The pattern of vertebral maturation and extended brain growth might reflect the broad Neandertal body form and physiology, rather than a fundamental difference in the overall pace of growth in Neandertals.

Science, this issue p. 1282